MASTER

INTERNAL TRANSMITTAL AUTHORIZED

X-822

OAK RIDGE NATIONAL LABORATORY
Operated by
UNION CARBIDE NUCLEAR COMPANY
Division of Union Carbide Corporation
UCC
Post Office Box X
Oak Ridge, Tennessee

[redacted]

ORNL
CENTRAL FILES NUMBER
59-6-18

COPY NO. 8

R-9435

DATE: June 2, 1959

SUBJECT: ORIC R-F Model III Progress Report

TO: Distribution

FROM: R. E. Worsham and S. W. Mosko

Distribution

1. R. H. Bassel
2. B. C. Behr
3. R. S. Bender
4. C. J. Borkowski
5. G. L. Broyles
6. J. A. Elkins
7. J. L. Hamilton
8. C. S. Harrill
9. F. T. Howard
10. E. D. Hudson
11. R. J. Jones
12. R. S. Livingston
13. R. S. Lord
14. J. E. Mann
15. F. W. Manning
16. M. B. Marshall
17. J. A. Martin
18. W. L. Morgan
19-28 S. W. Mosko (10)
29. M. E. Ramsey
30. E. G. Richardson, Jr.
31. A. W. Riikola
32. J. A. Russell
33. L. B. Schneider
34. W. R. Smith
35. A. H. Snell
36. J. A. Swartout
37-39. H. K. Walker (3)
40. A. M. Weinberg
41. T. A. Welton
42. W. H. White, Jr.
43. H. N. Wilson
44-53. R. E. Worsham (10)
54. N. F. Ziegler
55. A. Zucker

56. G. J. Berta
57. T. E. Bridge
58. H. R. Cloak
59. P. P. Febbo
60. H. H. Hassiepen
61-62. F. J. Knoll(2)
63. L. H. Jackson
64. W. E. Kunz

65. H. G. Blosser
66. B. L. Cohen

67. Laboratory Records

NOTICE

DISCLAIMER

DISCLAIMER

ORIC R-F MODEL III PROGRESS REPORT

R. E. Worsham and S. W. Mosko

The ORIC (Oak Ridge Relativistic Isochronous Cyclotron) radio-frequency system for which Model III represents the resonator is the third system which has received enough consideration to warrant construction of a model. The purpose of the model is to check the calculations for the frequency range and excitation power of the resonator. After an introductory description of the r-f system and model, the detailed calculations of the properties of the model will be given followed by the data from measurements of the model characteristics.

The general specifications within which the r-f system must fit are listed in Table I.

Table I: General Specifications for ORIC R-F System

Frequency range	7.5 to 22.5 Mc/s, cont. adj.
Frequency stability	1 part in 10^5, min.
Voltage gain/turn	200 kev (for singly-charged ions).
Orbit diameter	63 in.
Dee aperture	1.875 in.
Dee-to-liner clearance	1.5 in., max.
Maximum beam power	75 kw.
Regulation of dee voltage	1 part in 10^3, tentative.

In addition to these requirements, the inside of the liner, because of valley coils and circular trimming windings, should be flat allowing no additional dee-to-liner clearance in the valleys. Further, the time permitted for changing the r-f frequency should be, at most, a few minutes, since the cyclotron is designed for variable energy and because of the operating cost which makes a maximum innage essential.

Originally, in the r-f design, the voltage gain/turn was arbitrarily set at 400 kev. With increasing knowledge of the beam deflection mechanism and orbit properties in general, the threshold voltage has since been estimated as 137 kev/turn[(1)]; therefore, the value of 200 kev/turn would appear to be adequate and makes possible a simpler resonator with lower power loss, lower stored energy, apparently simpler mechanical construction, and, altogether, greater reliability than the earlier r-f systems considered for ORIC.

The dee-to-liner clearance was chosen as 1.5 in., a spacing which is capable of holding a peak r-f voltage of 100 kv reliably under operating conditions. Sections through the magnetic gap are shown in Figs. 1 and 2. On these drawings most of the dimensions are tentative and will be revised as necessary with progress in design.

Finally, consider Model III; a drawing showing the top and side views with the principal dimensions is shown in Fig. 3. Photographs of the model are Figs. 4 and 5. The model, which is quarter-scale, is constructed from wood covered with 4-mil copper foil on all inner surfaces. The outer tube in which the shorting plane travels was made, because of

[1] H. G. Blosser, ORNL-CF-59-5-59.

UNCLASSIFIED
ORNL-LR-DWG 34924

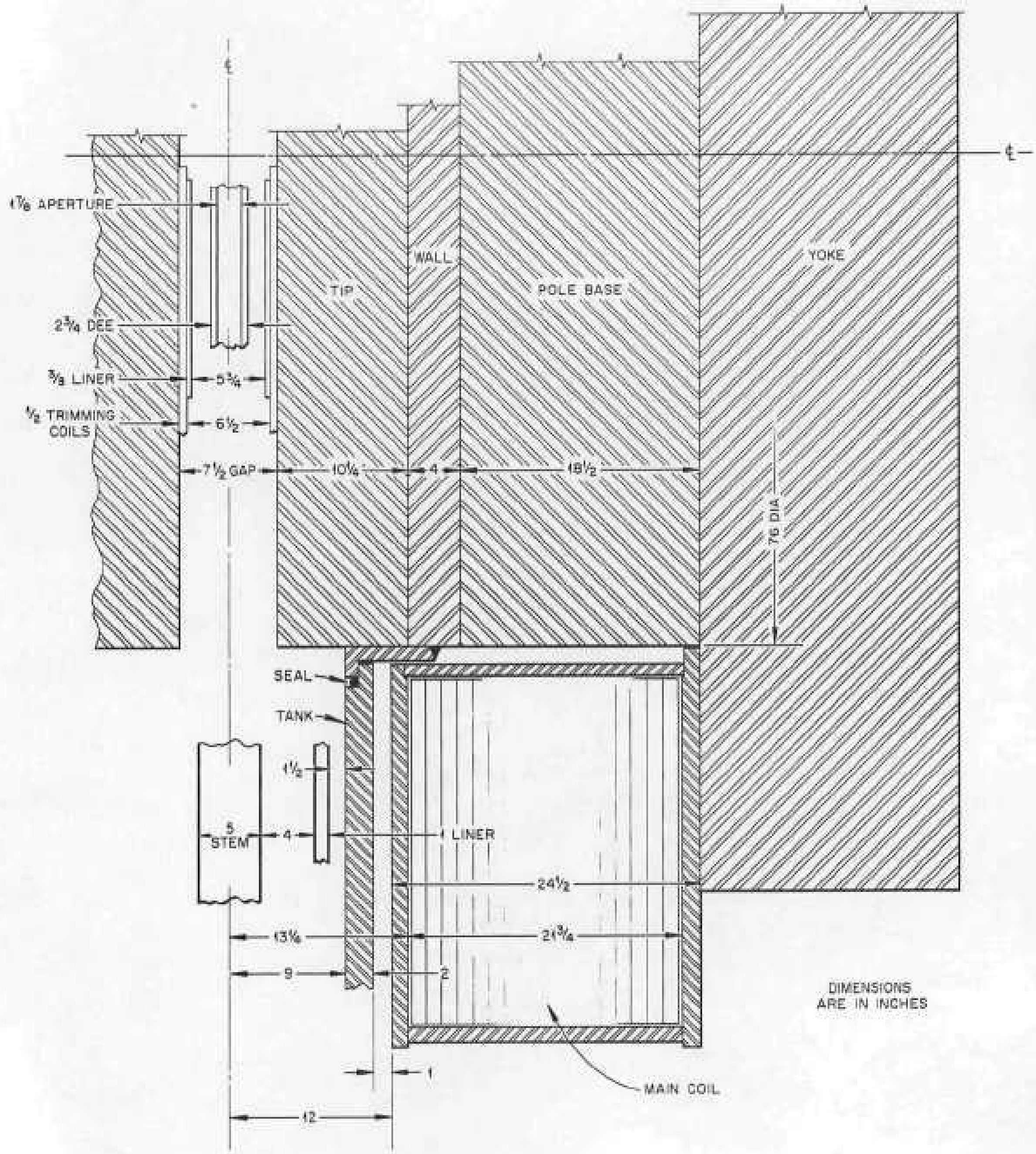

Fig. 1. Horizontal Section with Assigned Dimensions.

UNCLASSIFIED
ORNL-LR-DWG. 30818 R

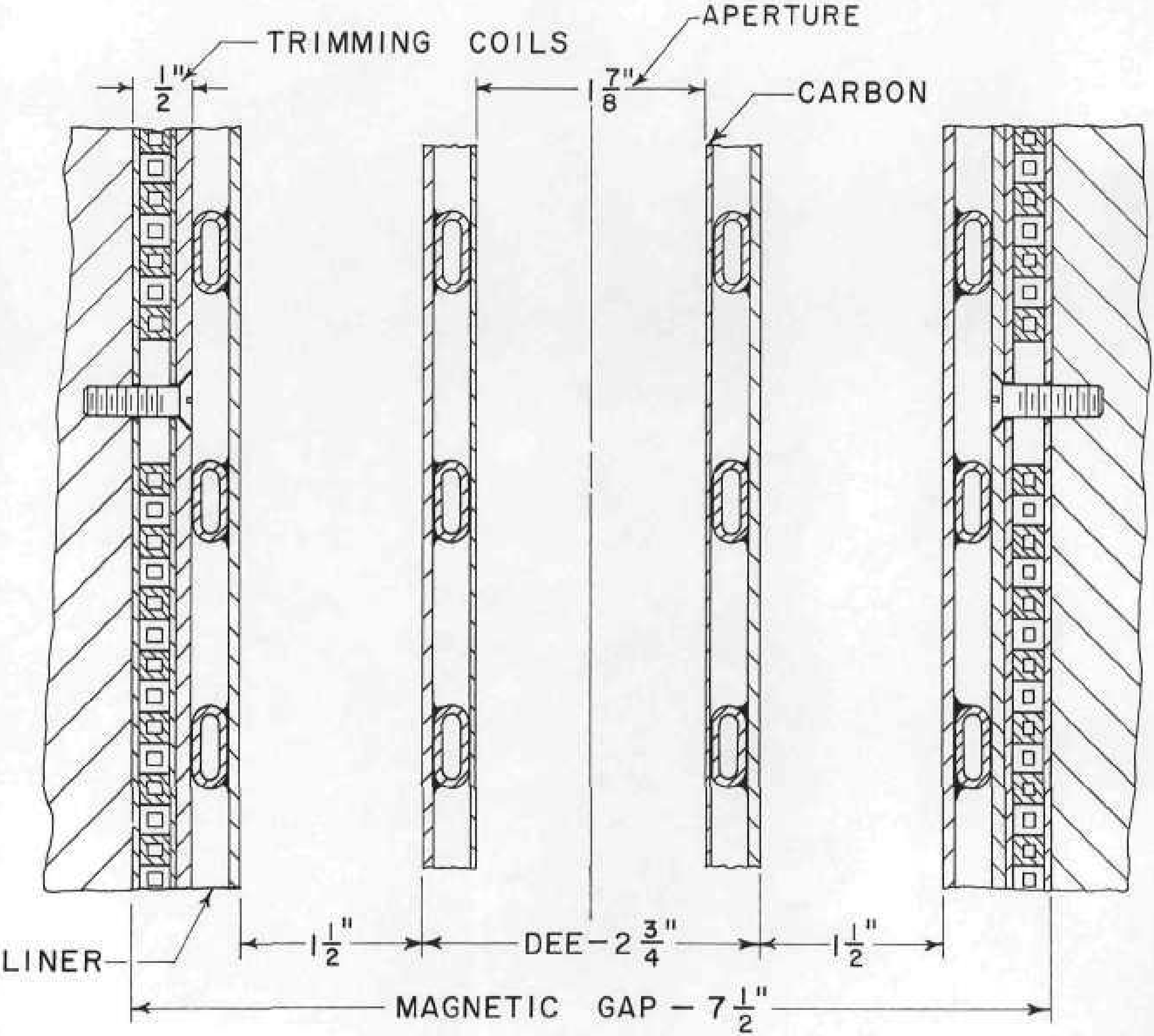

Fig. 2. Spacing of Dee and Liner in Magnetic Gap.

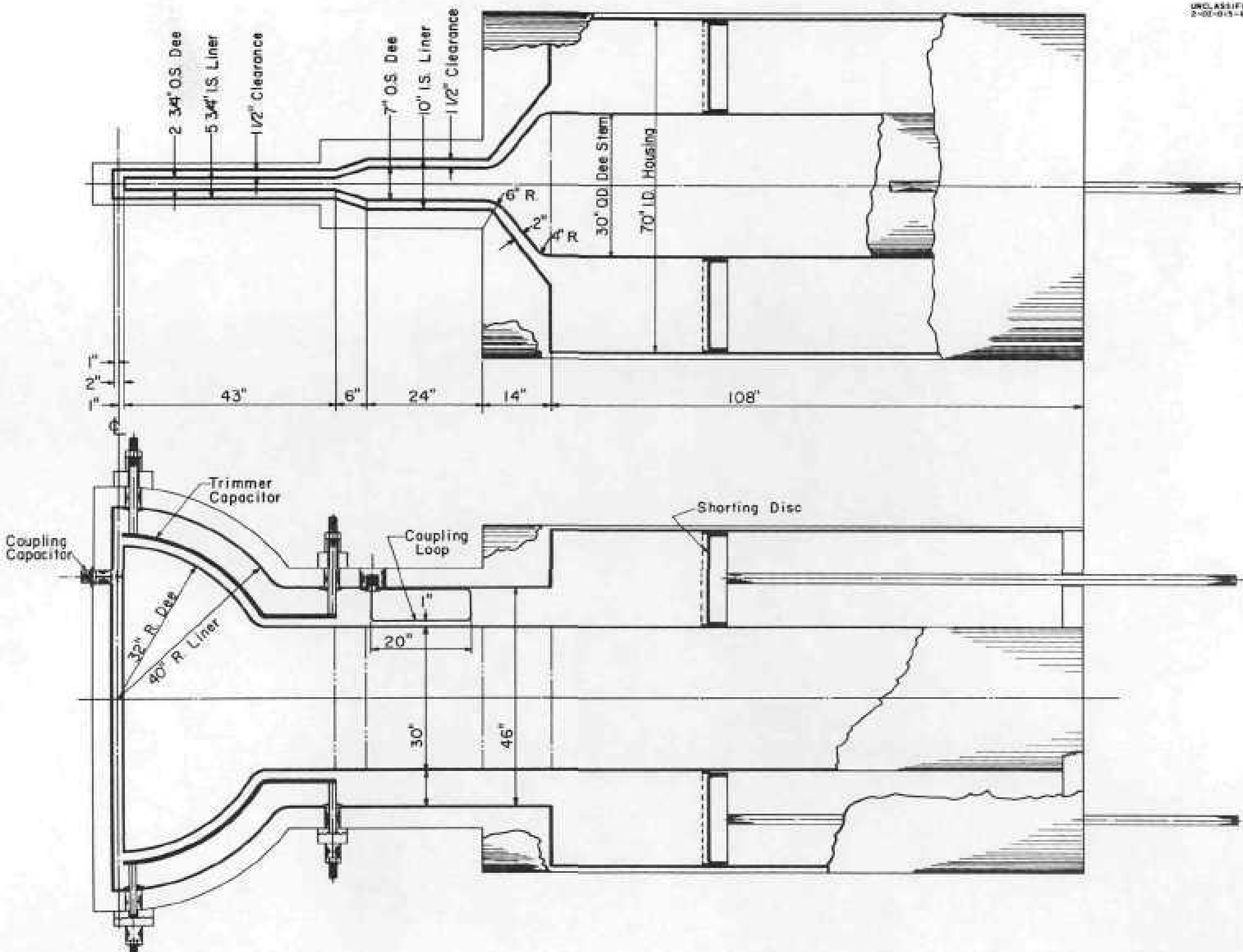

Fig. 3. Top and Side Views of Model III.

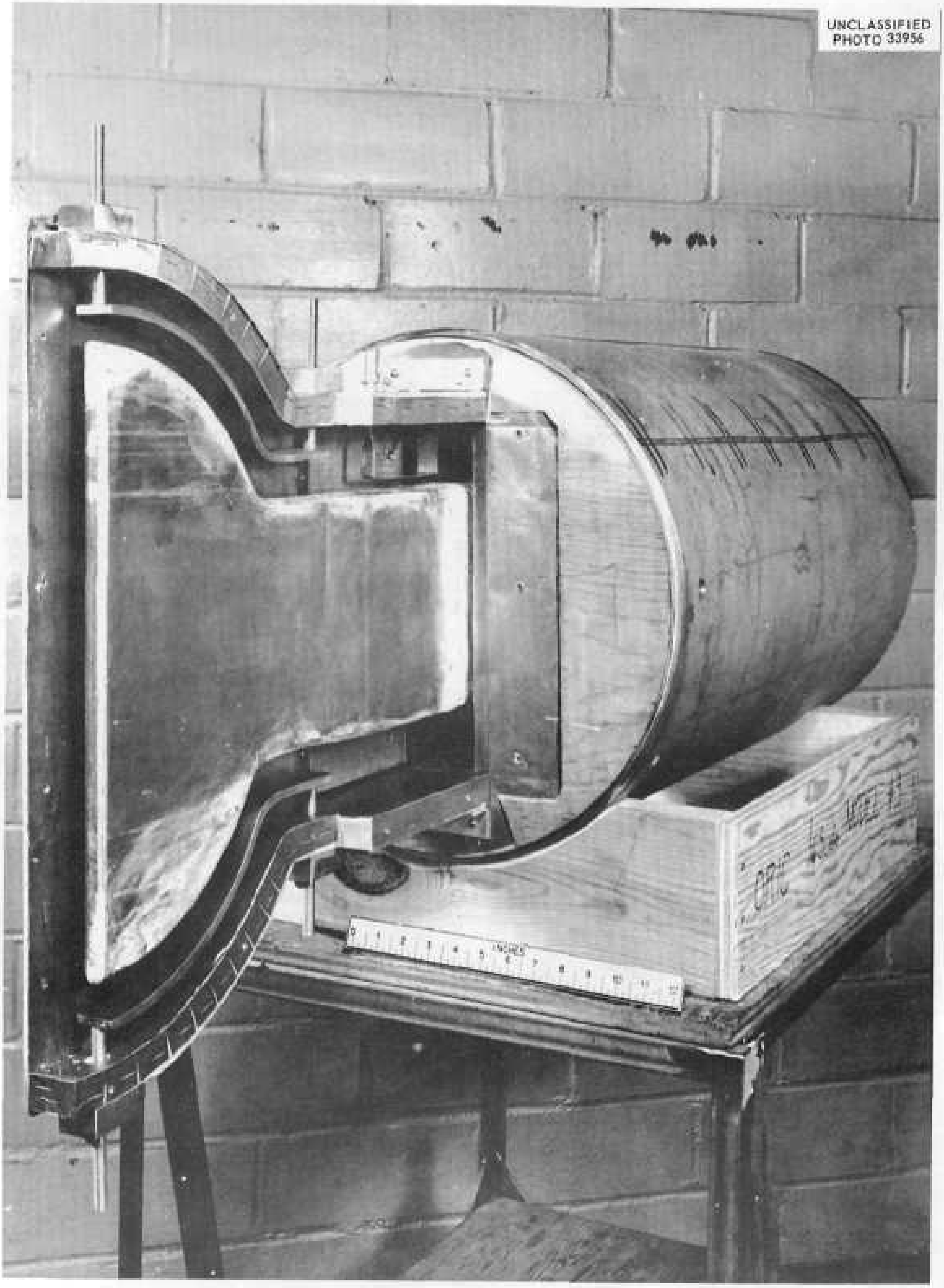

Fig. 4. R-F Model III.

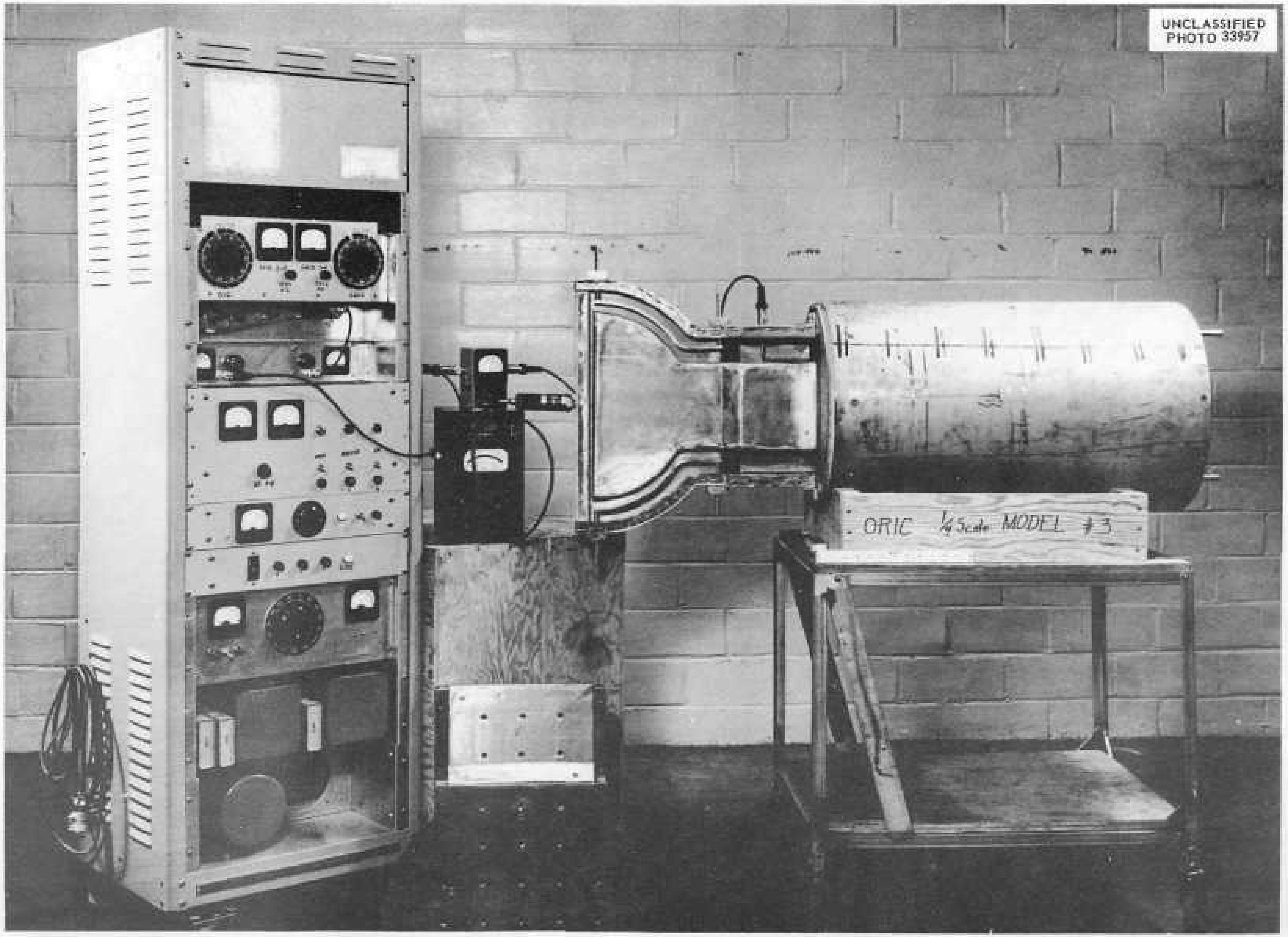

Fig. 5. R-F Model III.

availability, of an 18-in. OD stainless steel pipe. Copper foil was then cemented to the inside of the tube. For electrical contact, the shorting plane inner and outer edges were lined with finger stock. An item not included on the model, but planned for the full-scale machine is plates which would allow motion of the liner adjacent to the dee stem. This variation of stem characteristic impedance would be used for medium-coarse tuning.

PREDICTED MODEL-III CHARACTERISTICS

Computation of Characteristic Impedance

The characteristic impedance of a lossless transmission line is given by

$$Z_o = \sqrt{\frac{L}{C}},$$

where L is the series inductance per unit length, and C is the shunt capacity per unit length of line.

The velocity of propagation in a lossless transmission line is

$$v = \frac{1}{\sqrt{LC}} .$$

In air or vacuum, v is 3×10^8 meters/sec.

Thus:

$$v^2 = \frac{1}{LC}$$

$$L = \frac{1}{v^2 C} .$$

If we substitute this in the impedance equation, we get

$$Z_o = \frac{1}{vC} .$$

Now we can find the characteristic impedance for a transmission line if we know the shunt capacity per unit length.

The dee and the flat sections of the dee stem appear as a center plate in a parallel plate condenser. The capacity of a parallel plate condenser, neglecting fringing, may be found from

$$C = \frac{\epsilon_o \times A}{\delta} ,$$

where C is capacity in farads, A is the plate area in meters^2, δ is the distance between plates in meters, and $\epsilon_o = 10^{-9}/36\pi$ farads/meter. Since there are two dee and liner surfaces, the capacity for a given section will be:

$$C = 2\,\frac{8.85 \times A}{\delta}\ \mu\mu f$$

When the dee and dee stem are treated as a transmission line, the capacity per meter length C/m will be:

$$C/m = \frac{8.85 \times (2A)}{\delta \cdot \ell}$$

ℓ is the length of the section along the center axis of the transmission line.

Fringing

Before proceeding with the computation of Z_o, we must account for the increased capacity of the dee and stem caused by the fringing field. According to Smythe(2) the fringing causes an apparent increase in the width of the center plate of a three-plate condenser given by

$$\Delta Y = \frac{2}{\pi}\left[B \ln\left(\frac{2B-A}{B-A}\right) - A \ln\left(\frac{A(2B-A)^{1/2}}{B-A}\right)\right]$$

where ΔY is the apparent increase in width of the center plate, 2A is the thickness of the center plate, and 2B is the separation of the outer plates.

In Fig. 6, the dotted line outside the perimeter of the dee and stem encloses the apparent surface area which is used in computing Z_o. In the

[2] Smythe, W. R., Static and Dynamic Electricity, 1st Edition, McGraw-Hill, New York, p. 104.

UNCLASSIFIED
ORNL-LR-DWG 38661

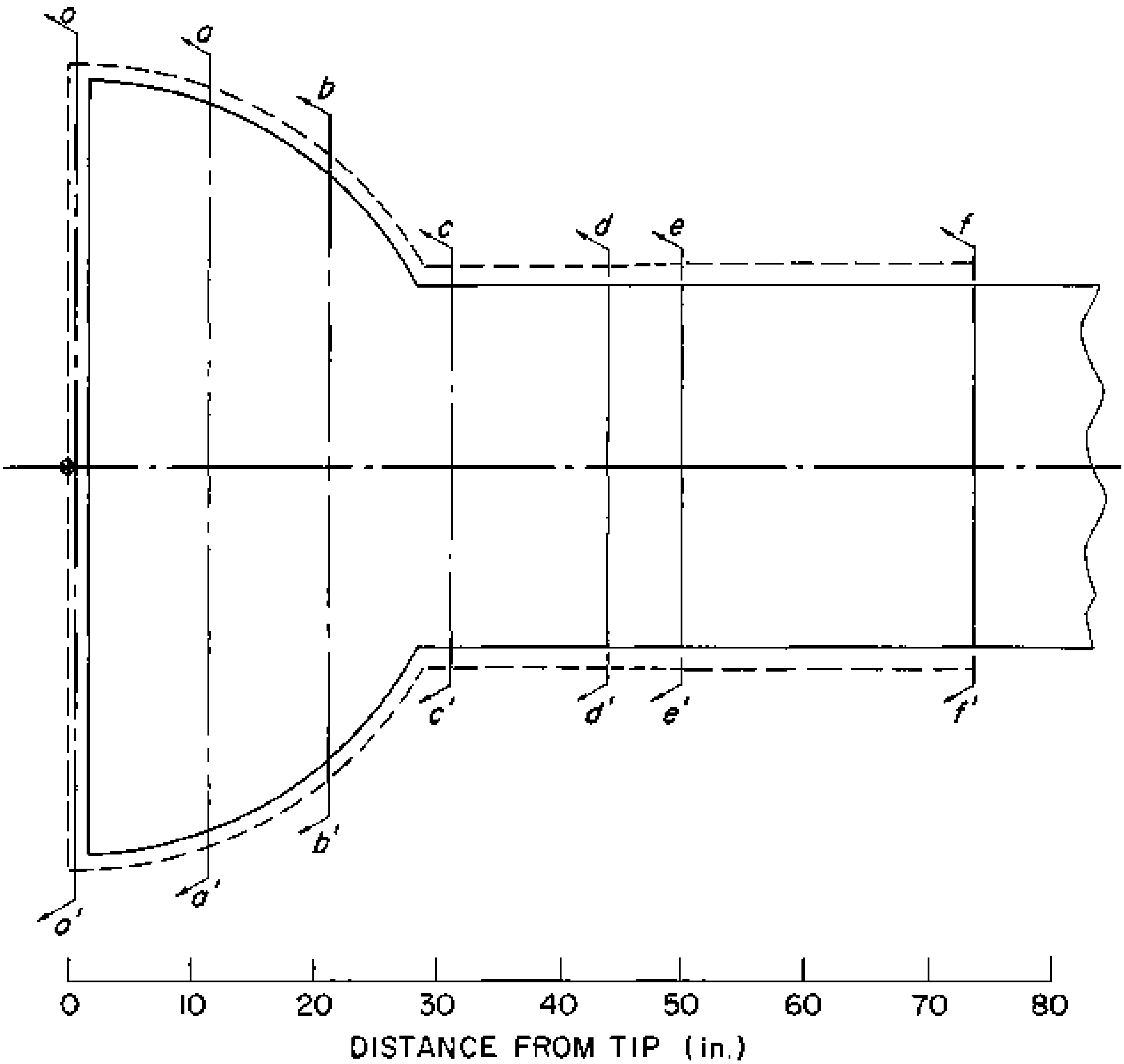

Fig. 6. Dee and Stem Showing Fringing Area and Sections of Non-Uniform Line.

section from d-d' to the dee tip, the fringe is 1.6-in. wide. For the remaining flat section of the dee stem, the fringe is 1.7-in. wide.

Computations

The constants which have been computed for several sections of the dee stem are shown in Table II. The characteristic impedance data are plotted in Fig. 7.

Table II: Constants of the Sections of Dee and Stem

Section (See Fig. 6)	(Total Area) 2A $(in.)^2$	(Separation) δ (in.)	(Length) (in.)	C/m ($\mu\mu f$/meter)	Average Z_0 for section Z_0 (Ω)
a-a'	1522	1.5	11.6	775	4.30
b-b'	1160	1.5	10.0	684	4.87
c-c'	842	1.5	10.0	497	6.71
d-d'	863	1.5	13.0	393	8.48
e-e'	477	1.5	7.2	391	8.48
f-f'	1598	1.5	24.0	393	8.48

The characteristic impedance of the dee stem in the region following section f-f' is somewhat uncertain. If the stem-to-liner clearance remains constant at 1.5 in. in this region, Z_0 will decrease as the cross section perimeter of the dee stem increases. A minimum value of Z_0 occurs at the point where the dee stem becomes fully cylindrical. This minimum value of Z_0 may be estimated from the equation for the

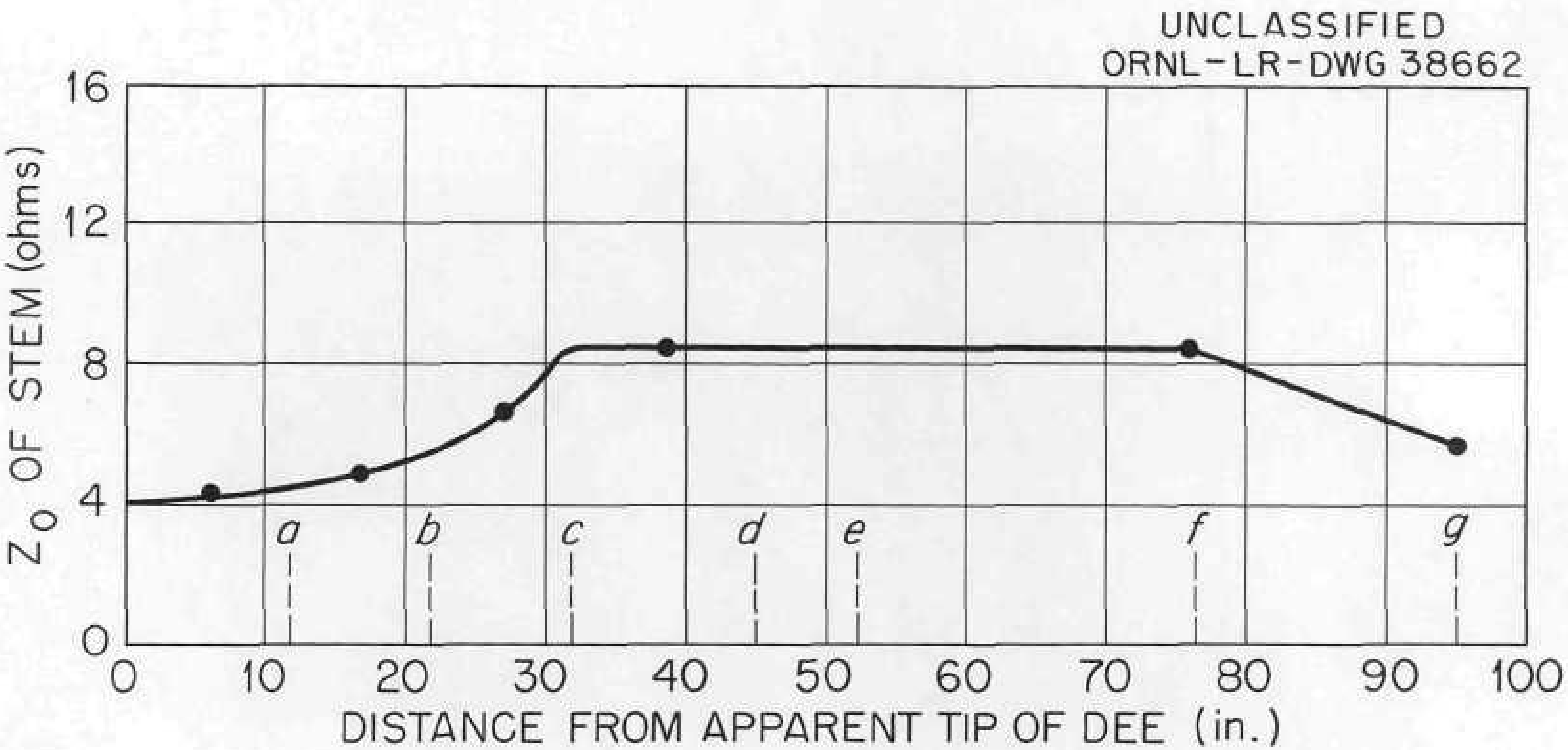

Fig. 7. Characteristic Impedance Along Dee and Stem.

characteristic impedance of a coaxial line.

$$Z_o = 60 \ln \frac{D}{d} \qquad D = \text{outside conductor ID.}$$

$$= 60 \ln \frac{33}{30} = 5.72\ \Omega. \qquad d = \text{inside conductor OD.}$$

The remainder of the dee stem and the liner is cylindrical and coaxial with a diameters ratio of $\frac{70}{30}$.

$$Z_o = 60 \ln \frac{70}{30} = 50.8\ \Omega.$$

The characteristic impedance of the region within a few inches of the shorting plane will be considerably less than 50.8 Ω, however.

Voltage Standing Waves and Current Standing Waves

The standing waves along the dee stem must be known to find the required position of the shorting plane; they are also needed for computing power losses. The standing waves may be computed from the transmission lines equations:

$$v_R = v_s \cos \frac{2\pi s}{\lambda} + jI_sZ_o \sin \frac{2\pi s}{\lambda}$$

$$I_R = I_s \cos \frac{2\pi s}{\lambda} - \frac{v_s}{jZ_o} \sin \frac{2\pi s}{\lambda}.$$

v_R = voltage at point of interest along line.

v_s = voltage some distance "s" down line.

I_R = current at point of interest.

I_s = current some distance "s" down the line.

λ = wave length of the standing wave = $\frac{c}{f}$.

In computing the magnitude of the standing waves at various frequencies, it is assumed that the system is in resonance, and that the voltage on the dee is 100-kv peak or 70.7 kv (rms). Since the characteristic impedance of the line is not uniform, the VSW and CSW must be determined at several incremental distances along the line. The voltage and current standing-wave data for the resonator are shown for several frequencies in Table III.

The position of the shorting plane required for a given frequency is found as follows: When the shorting plane is very close to the forward end of the cylinder, the length of line in the cylindrical region is approximately equal to the difference in liner and stem radii, or a length of 20 inches. The characteristic impedance of the region will depend upon the clearance between the shorting plane and the end of the cylinder. At the upper end of the resonator's frequency range, we may solve for the shorting plane position by assuming S = 20 in. in the VSW equation and solving the equation for Z_o. The voltage node should be located near the outer edge of the shorting plane. The distance between the shorting plane and the front end of the cylinder will be approximately that distance which will give the required Z_o.

At low frequencies, when the shorting plane is near the rear of the cylinder, the cylindrical section behaves like a 50-ohm coaxial line. Fringing will cause low impedance at the shorting plane, so that its electrical length between the center and outer conductor will appear to be very short. When the voltage standing wave equation is solved for S in the cylindrical region, S will be the required distance from the shorting bar to the front end of the cylinder. A curve of frequency vs shorting-plane position is shown in Fig. 8. The shorting plane position

Table III: Computed Values of the Voltage and Current Standing Waves

Frequency Mc/s	Distance from Dee Tip (in.)	V (kv)	I (ka)	Z_0 (Ω)	Shorting Plane Distance from Front End of Cylinder (in.)
	0.0	70.7	0.00	-	
	10.0	70.1	2.00	4.30	
	20.0	68.3	3.78	4.75	
22.5	30.0	64.9	5.09	6.20	5
	70.0	37.8	8.18	8.25	
	76.0	32.8	8.50	8.25	
	95.0	17.4	9.37	7.00	
	0.0	70.7	0.00	-	
	10.0	70.3	1.57	4.30	
	20.0	69.2	2.99	4.75	
18.0	30.0	67.1	4.05	6.20	11
	76.0	46.5	7.13	8.25	
	95.0	36.7	8.23	7.00	
	0.0	70.7	0.00	-	
	30.0	69.2	3.29	5.10	
13.0	76.0	57.2	5.75	8.25	24
	95.0	51.5	6.78	7.00	
7.5	0.0	70.7	0.00	-	78
	95.0	65.7	4.49	5.74	

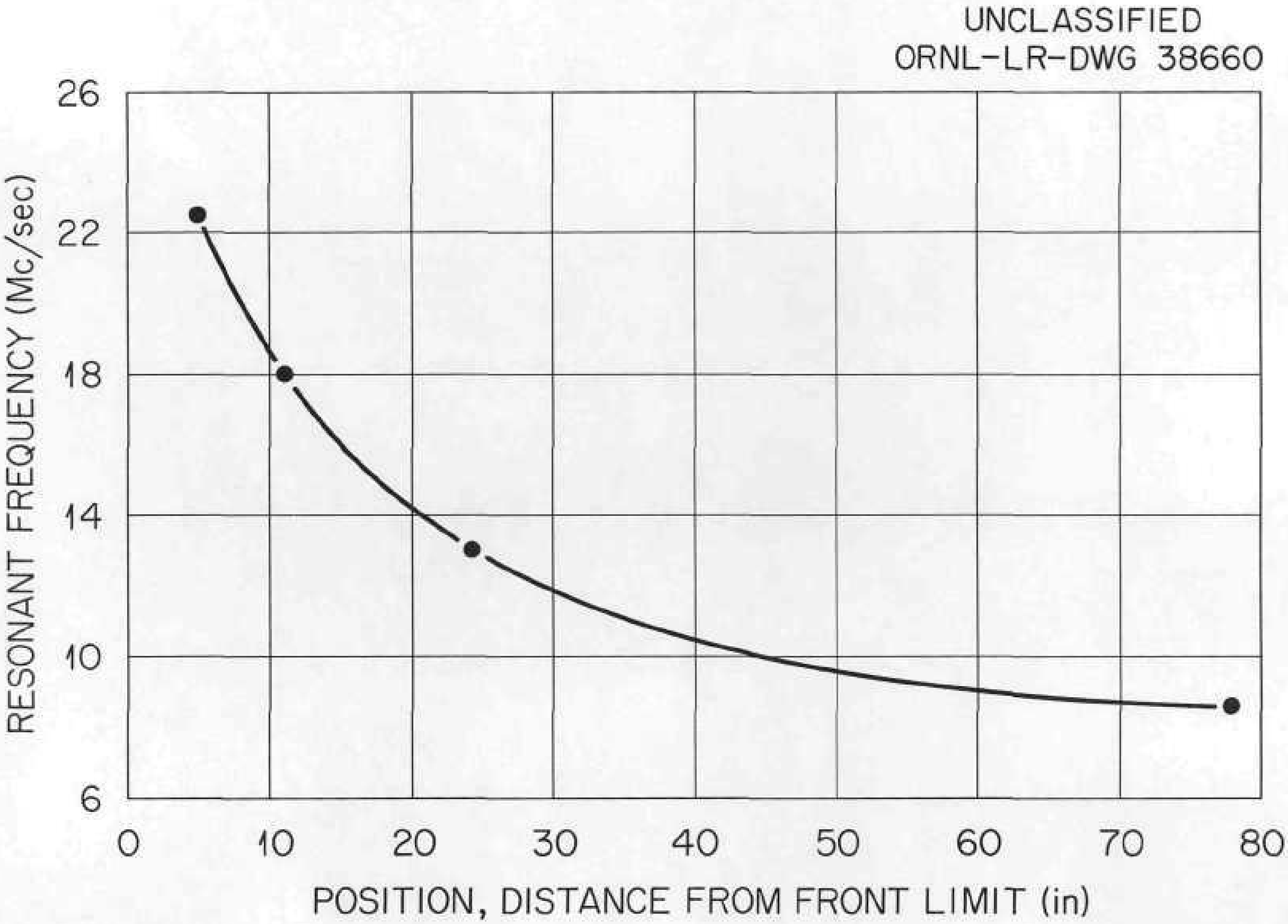

Fig. 8. Resonant Frequency vs Shorting Bar Position.

is given by its distance from the front end of the cylindrical line section.

Power Losses

The I^2R power loss may be determined if we know the current densities at every point in the resonant system. The total current at a point along the dee stem may be found on the CSW curve. The current distribution at any point may be found by considering the geometry of the cross section of the dee stem perpendicular to the current path.

Due to skin effect, the current will be concentrated on the conductor surface. Also, the current will tend to concentrate in the regions of highest capacity. Thus, for the typical cross section in Fig. 9, the current will be assumed to be concentrated in cross sectional area of $(\overline{ab} + \overline{cd} + \overline{ef} + \overline{gh}) \cdot \delta/2$, where δ is the skin depth.

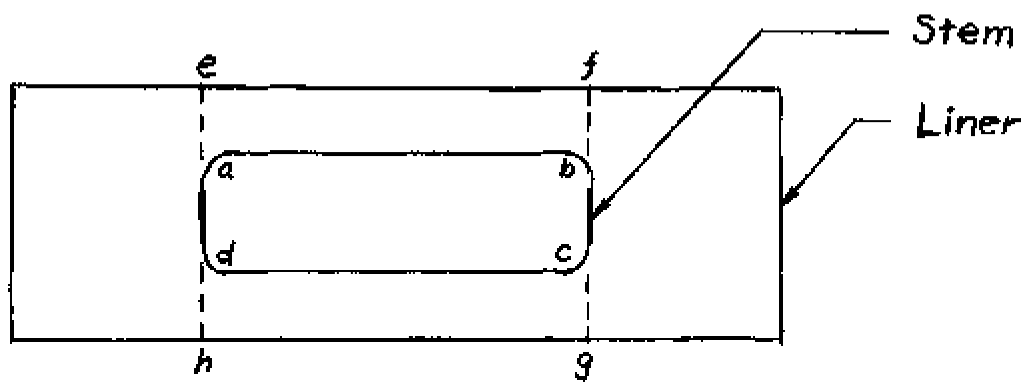

Fig. 9

The maximum power loss will occur at the maximum operating frequency, since the current densities in the shorting plane region increase with frequency. The effects of longer line length at lower frequencies are more than offset by the decrease in current and increase in skin depth.

Power Loss Computations

The voltage and current standing waves are plotted in Fig. 10, and the effective cross section and resistance is plotted in Fig. 11. The data from these curves are tabulated for several increments of length in Table IV.

The power loss in each incremental area is I^2R. The average value of I^2 is approximated by the formula

$$I^2 = \frac{I_1^2 + 2I_2^2 + \ldots . I_n^2}{2(n-1)}$$

where I_1 and I_n are end points, and I_2 and I_3 ..... I_{n-1} are taken at equally spaced intervals. The values required for computation are:

Resistance of copper = 1.72×10^{-8} ohm-meter

The skin depth for copper = $\delta = \frac{6.62 \times 10^{-2}}{\sqrt{f}}$ meters.

Therefore, at 22.5 Mc/s, the resistance of a section of the dee or stem is given by

$$1.214 \times 10^{-3} \frac{(\text{length})}{(\text{width})} \text{ ohms}$$

According to Table IV, the total I^2R power loss to be expected when the resonant system operates at 22.5 Mc/s and 100 kv on the dee is approximately 180 kw. This figure is based on uniform current distribution in the transition region where the dee stem cross section changes from elliptical to cylindrical. Since the r-f current in this region is quite high, non-uniform current distribution would cause a considerable increase in power loss. Consequently, a study of current distribution was made to determine what power loss increase should be expected.

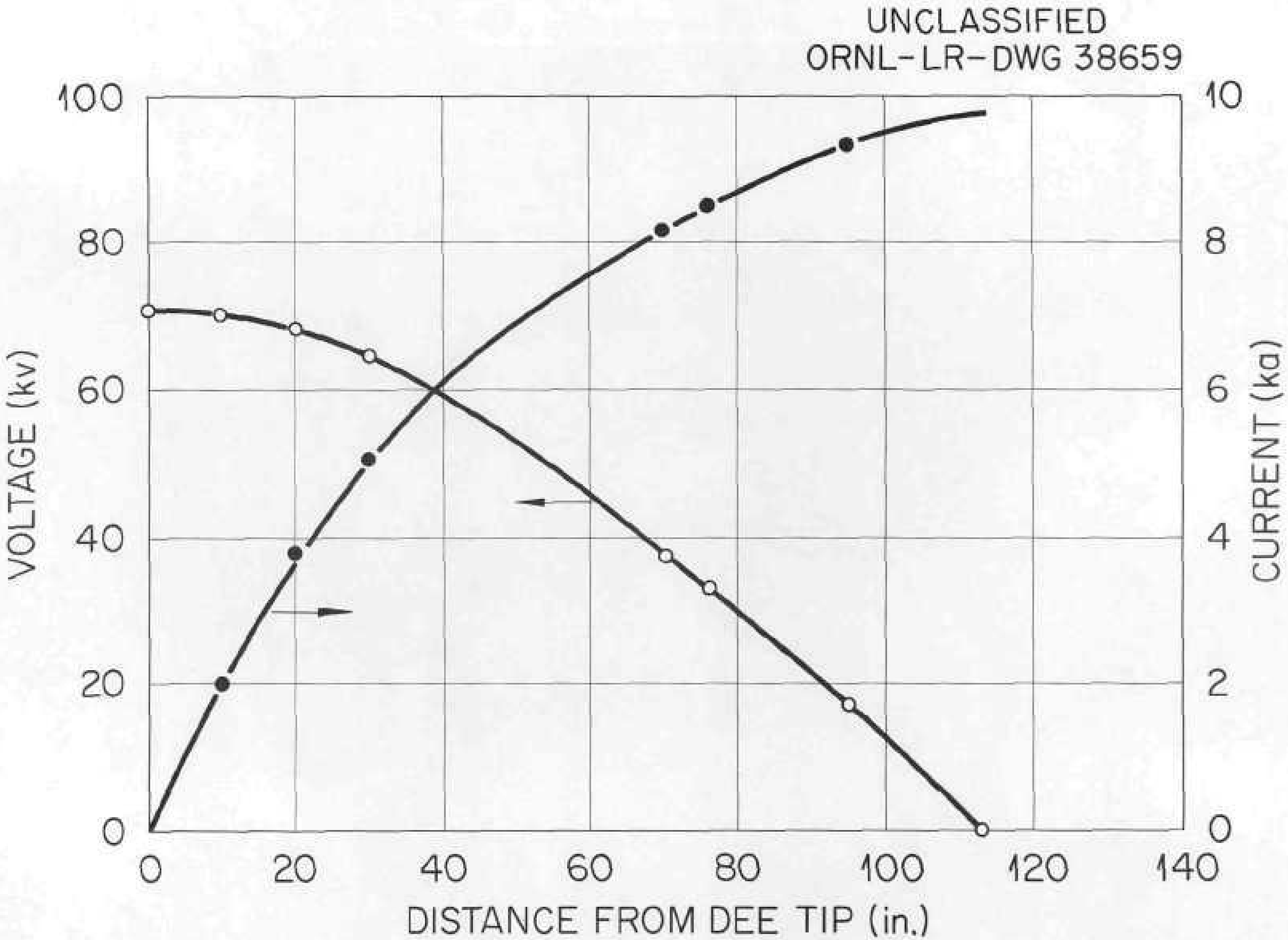

Fig. 10. VSW and CSW at 22.5 Mc/sec.

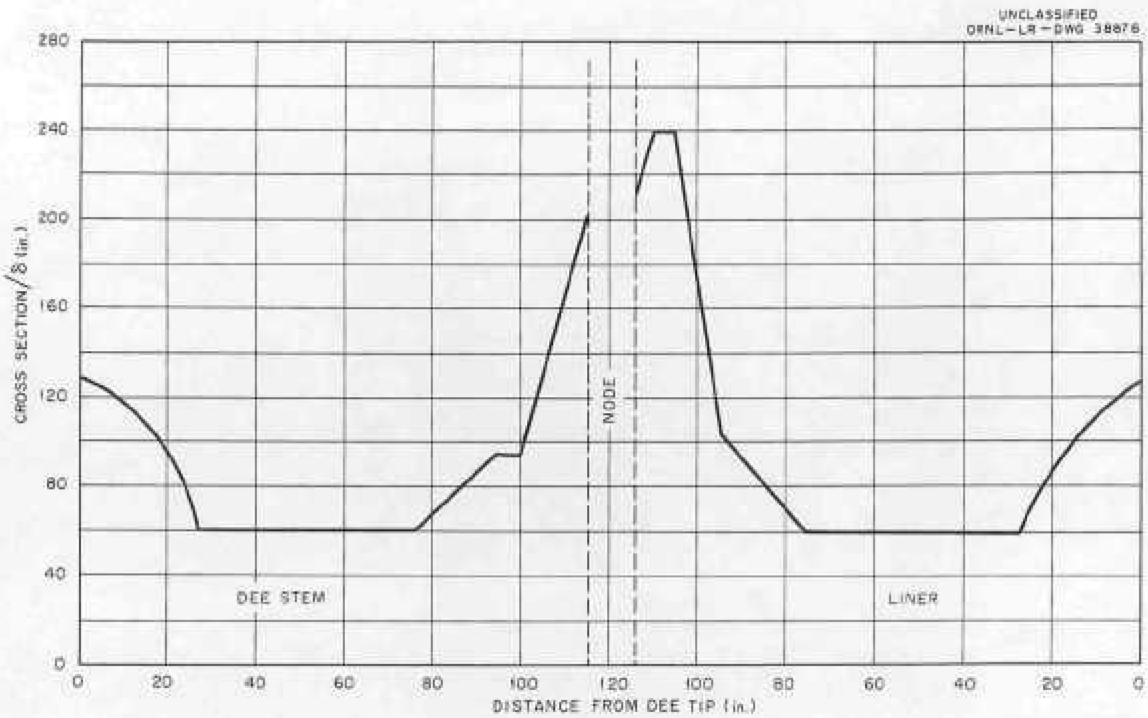

Fig. 11. Effective Cross Sectional Area of Current Path.

Table IV: Computation of Power Losses

	Distance from Dee Tip (in.)	Cross Section/ δ	Resistance per 10 in. length (ohms x 10^5)	Average I^2 $(ka)^2$	Power (kw)
Stem	10	116	10.46	4.1	0.429
	20	95	12.78	14.1	1.800
	30	60	20.23	26.0	5.26
	40	60	20.23	37.2	7.53
	50	60	20.23	47.7	9.65
	60	60	20.23	57.8	11.69
	70	60	20.23	66.5	13.45
	80	68	17.84	75.8	13.52
	90	85	14.28	84.8	12.11
	100	96	12.64	90.4	11.43
	110	170	7.14	94.4	6.74
Liner	110	218	5.57	94.4	5.26
	100	170	7.14	90.4	6.45
	90	92	13.19	84.8	11.19
	80	70	17.34	75.8	13.14
	70	60	20.23	66.5	13.45
	60	60	20.23	57.8	11.69
	50	60	20.23	47.7	9.65
	40	60	20.23	37.2	7.53
	30	60	20.23	26.0	5.26
	20	95	12.78	14.1	1.80
	10	116	10.46	4.1	0.429

Total Power Loss: 179.5 kw

Study of Current Distribution

An approximate pattern of current distribution at various points along the transition region was obtained by studying the two dimensional flux pattern of electrodes with similar cross section to that of the stem and liner. The flux density at any point on the electrode surface is proportional to the current density at a corresponding point on the dee-stem cross section.

The flux patterns were obtained from an Analog Field Plotter(3); they are illustrated in Fig. 12.

The Flux Plotter data were used for plotting equipotential lines. Flux lines can easily be determined, since it is known that the flux density along a path perpendicular to the equipotential lines is inversely proportional to the clearance between the equipotential lines. Values of flux for increments of cross section were tabulated in Table V.

The expected power loss for a system with uniform current distribution is proportional to the square of the average value of incremental flux. The actual power loss is proportional to the average of the squares of the values of incremental flux. The increase in power loss resulting from non-uniform current distribution can be determined from

$$\% \text{ power loss increase} = (100)\,\frac{(\text{non-uniform loss})-(\text{uniform loss})}{(\text{uniform loss})}$$

According to Table V, the power loss increase for the three cross sections considered would be:

[3] G. E. Analog Field Plotter, Cat. # 112L152G1.

UNCLASSIFIED
ORNL-LR-DWG. 38875

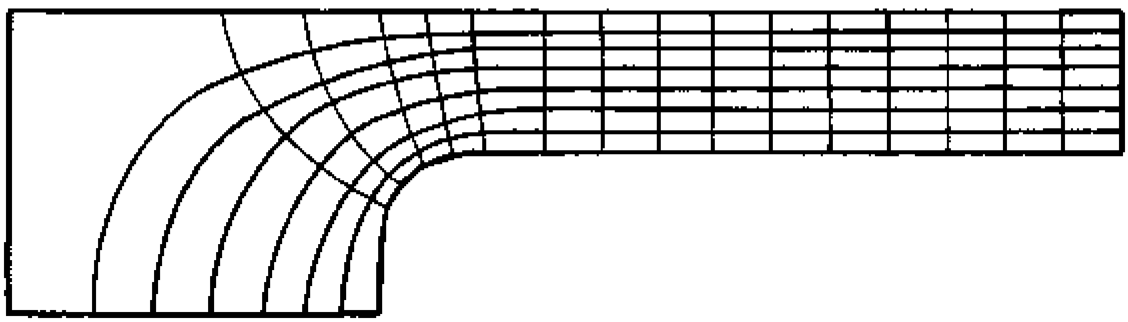

Fig. 12a. One-Fourth Cross Section Flux Path at Beginning of Transition Region 80 in. From Tip of Dee.

UNCLASSIFIED
2-02-015-688

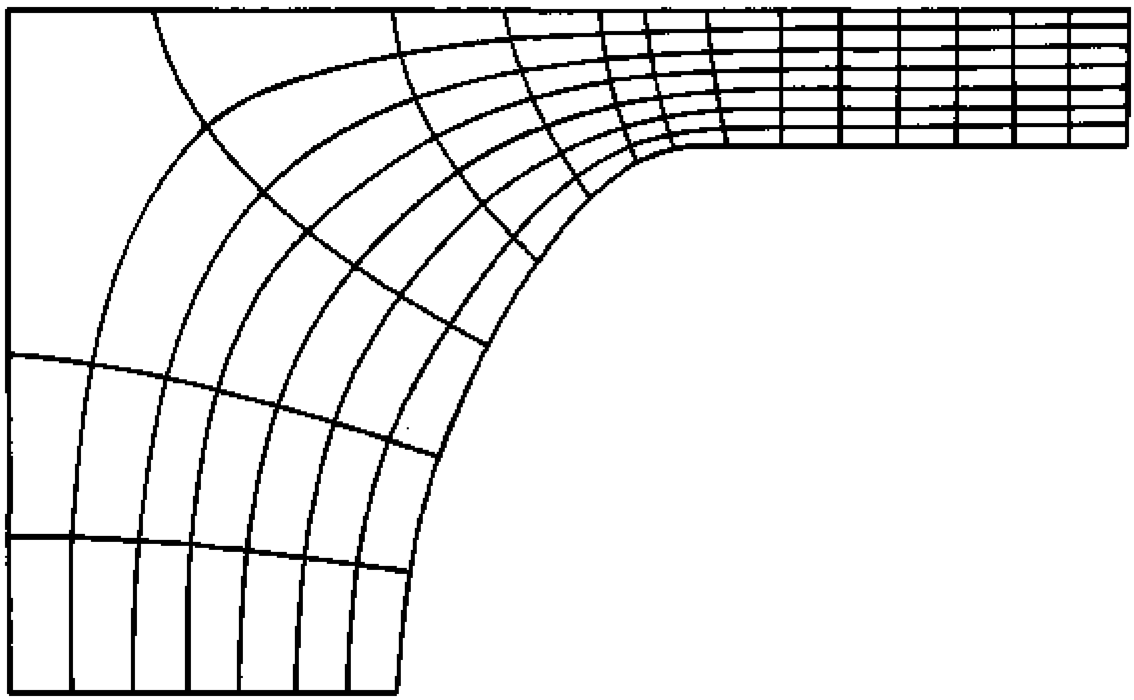

Fig. 12b. Flux Plot, 1/4 Cross Section Middle of Transition Region.

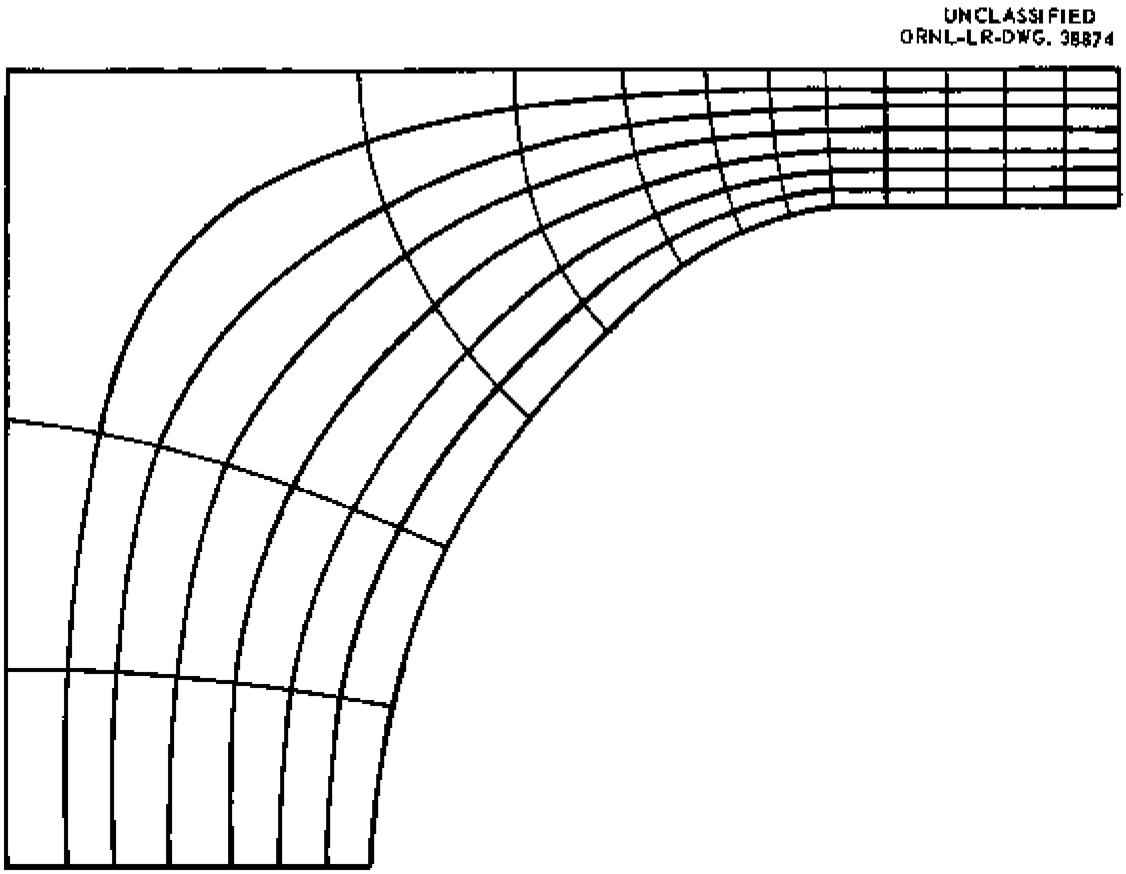

Fig. 12c. One-Fourth Cross Section Flux Plot Near End of Transition Region 87 in. Path Length From Tip of Dee.

Table V: Data from Flux Plots

	Clearance	Flux	$(\text{Flux})^2$	Clearance	Flux	$(\text{Flux})^2$	Clearance	Flux	$(\text{Flux})^2$
	.10	10.0	100.0	.10	10.0	100.0	.10	10.0	100.0
	.10	10.0	100.0	.10	10.0	100.0	.10	10.0	100.0
	.11	9.1	83.0	.12	8.3	69.0	.11	9.1	83.0
	.12	8.3	69.0	.21	4.8	23.0	.24	4.2	18.0
Liner	.31	3.2	10.0	.41	2.4	5.7	.54	1.9	3.6
	.78	1.3	1.7	1.02	1.0	1.0	1.08	0.93	0.9
	.61	1.6	2.6	.82	1.2	14.0	.99	1.0	1.0
	.48(.13)	2.1(.3)	4.4(.3)	.50	2.0	4.0	.54	1.9	3.6
				.35	2.9	8.3	.39	2.6	6.8
				.34(.35)	2.9(.35)	8.3(.35)	.32	3.1	9.6
Totals		44.1	368.0		43.6	328.0		44.7	327.0
	.10	10.0	100.0	.28	3.6	13.0	.25	4.0	16.0
	.10	10.0	100.0	.24	4.2	18.0	.28	3.0	13.0
Stem	.10	10.0	100.0	.18	5.6	31.0	.23	4.3	19.0
	.7	14.0	196.0	.06	17.0	289.0	.18	5.6	31.0
	.19(.6)	5.3(.6)	28.0(.6)	.10	10.0	100.0	.06	17.0	290.0
				.10	10.0	100.0	.10	10.0	100.0
				.10(.15)	10.0(.15)	100.0(.15)			
Totals		47.1	513.0		51.9	566.0		44.5	469.0

$(\text{Ave Flux})^2$	Liner	36.5	21.7	20.0
	Stem	104.0	71.1	55.0
Ave (Flux^2)	Liner	50.4	35.0	32.7
	Stem	112.0	92.0	78.2
Power Increase	Liner	38%	61%	64%
	Stem	8%	29%	42%
	Total	23%	45%	53%

a) 23%

b) 45%

c) 53%

When the resonator is operating at its maximum frequency, the current enters the shorting plane from the dee stem in two concentrated regions. The lowest impedance path from the dee stem to the liner is in a radial direction along the shorting plane. Consequently, the current in the shorting plane probably remains concentrated in two paths as shown in Fig. 13. The power loss increase in the shorting plane would then be similar to that in the nearest section of the transition region, or about 50%.

Referring back to Table IV, it can be seen that more than half the total power loss in the resonator occurs in the region near the shorting plane. A 50% increase in the power loss of this region would, therefore, increase the total power loss of the resonator by more than 25%. Therefore, a power loss of 230 kw should be expected when the resonator is operating at 22.5 Mc/s and 100-kv peak dee voltage.

UNCLASSIFIED
ORNL-LR-DWG. 38873

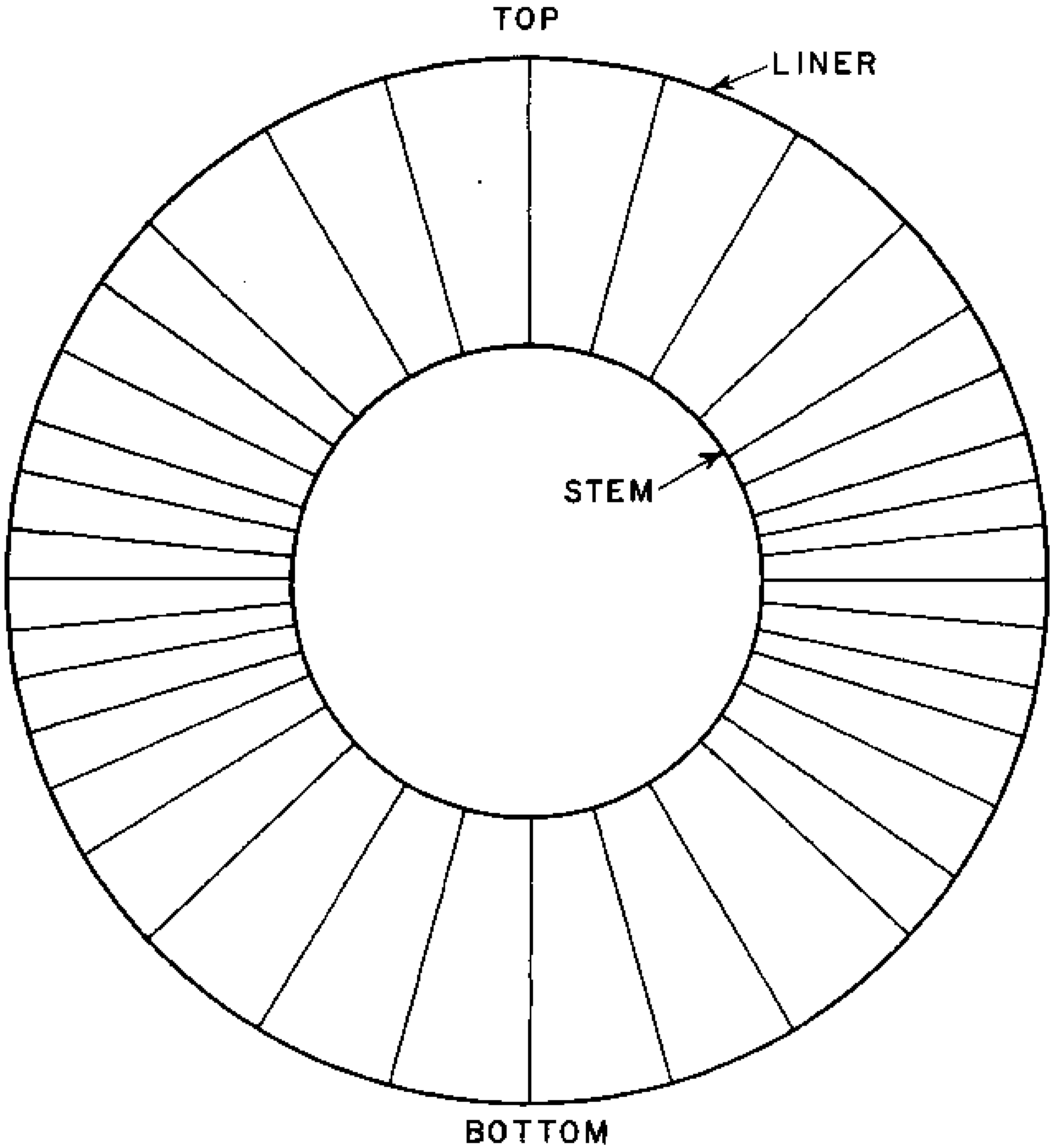

Fig. 13. Current Distribution in Shorting Plane.

OBSERVED MODEL-III CHARACTERISTICS[4]

Tuning Range

A grid dip meter was used for measuring the resonant frequency at various shorting-plane positions. These data are shown on the curve in Fig. 14. When the plane is 1/8-in. from the front end of the cylindrical section, the resonant frequency of the model is 90 Mc/s, which corresponds to a full-scale frequency of 22.5 Mc with the shorting plane 1/2 in. from the front end. A resonant frequency of 30 Mc/s occurs when the shorting plane is 20 in. from the front end. This corresponds to a full-scale resonant frequency of 7.5 Mc with the shorting plane located 80 in. from the front end.

A set of fine-tuning condensers was installed along the periphery of the dee. These trimmers can be moved from a position with clearance of approximately 2 in. to a position with complete contact with the dee periphery. The system may be tuned from 88.5 to 90 Mc/s by moving the trimmers from 1/4-in. clearance to 1-1/2-in. clearance.

Measurement of VSW

Several holes were cut in the liner so that a VTVM probe could be inserted at points along the dee. The data obtained by VTVM measurements are plotted in Fig. 15 to show the VSW on the dee when the system is operating at 90 Mc/s. The voltage on the accelerating edge of the dee

---

[4] The data of this section were obtained from the model as shown in Figs. 4 and 5.

UNCLASSIFIED
ORNL-LR-DWG 38658

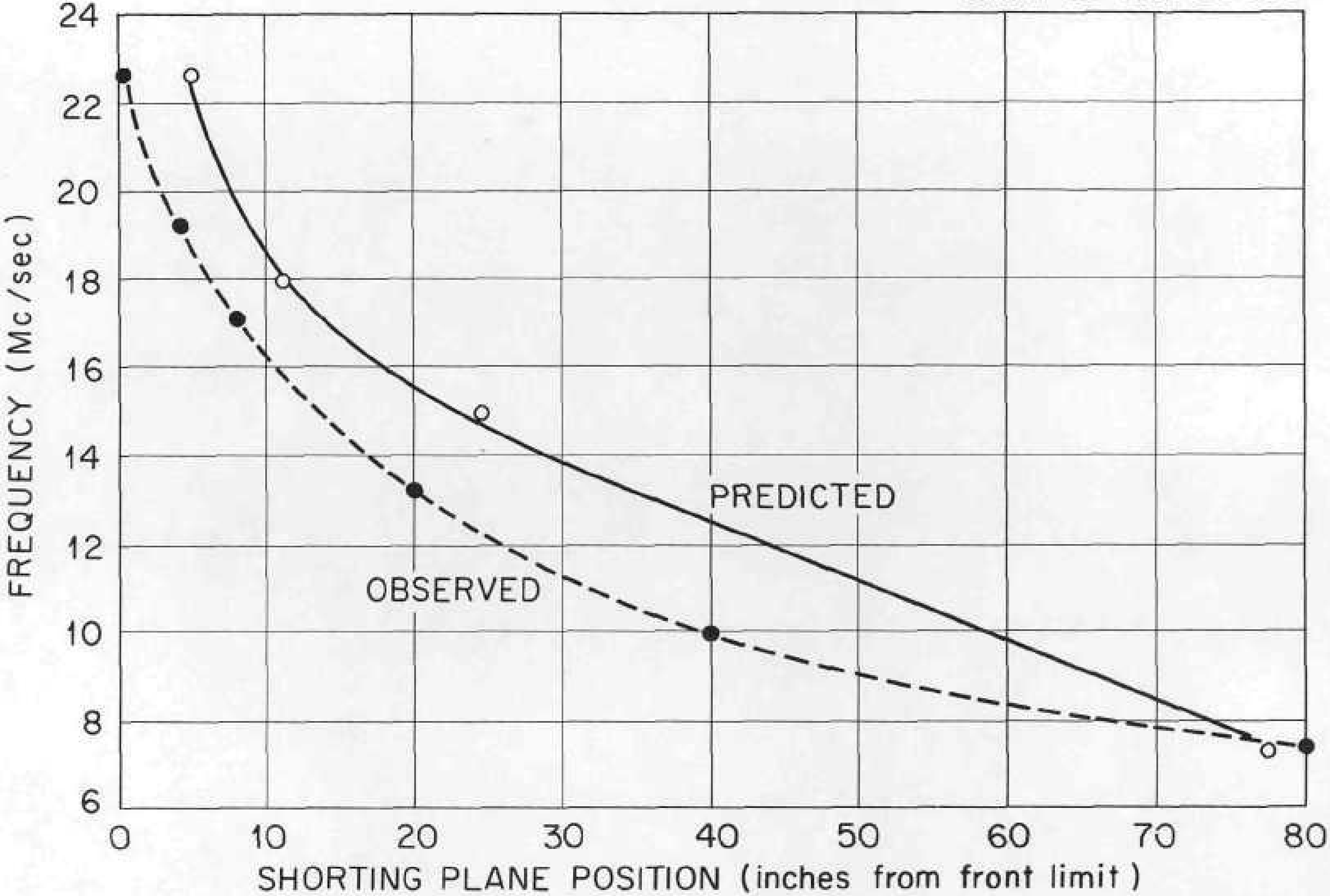

Fig. 14. Measured and Computed Frequency vs S.P. Position.

UNCLASSIFIED
ORNL-LR-DWG 38657

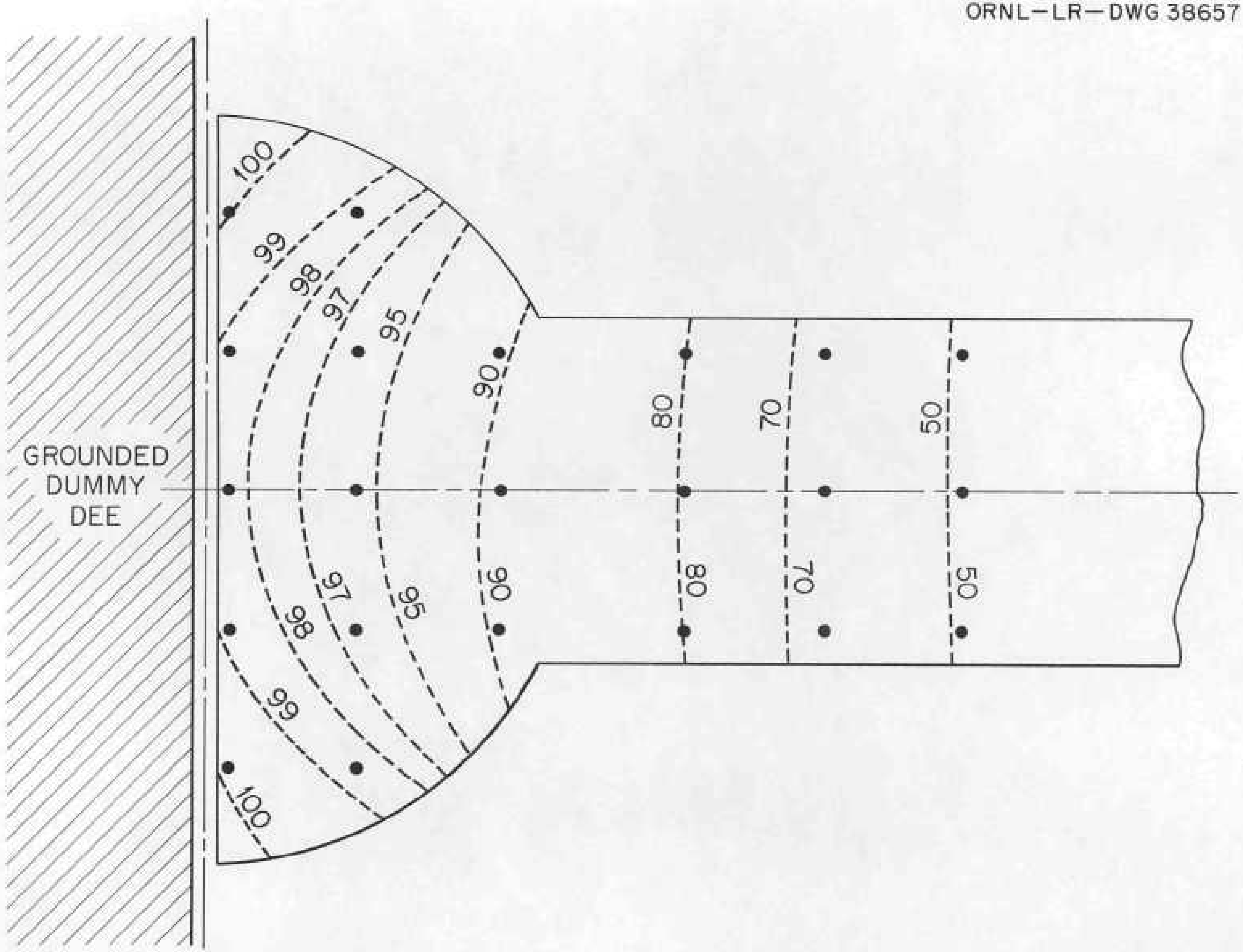

Fig. 15. VSW on Model III.

varies from 100 kv at large radius to about 98.5 kv at the center.

In Fig. 16, the observed VSW data are plotted along with the predicted VSW data. The deviation from the predicted curve shows that the maximum frequency of the model is lower than that which was expected.

Direct Power Input Measurement

Direct power input measurements were made on the model by placing in the input loop a directional-coupler type wattmeter which had been calibrated at a power level of 7.4 watts with a voltmeter and known load resistor. The wattmeter can read either forward or reflected power. The difference of the two readings is equivalent to the power loss in the resonator. The following data were obtained in a typical power measurement:

Frequency = 89.0 Mc/s

Dee voltage = 248 volts rms

Power loss = 7.89 watts.

The power loss on the full-scale machine operating at 100-kv peak dee voltage and a frequency of 22.3 Mc/s can be found by the relation:

$$P_{(\text{full scale})} = \left(\frac{P_{\text{model}}}{2}\right)\left(\frac{V_{\text{full scale}}}{V_{\text{model}}}\right)^2 .$$

The factor 2 enters because the model operates at four times the full-scale frequency, and skin depth varies with the square root of frequency. Thus the power loss in the full-scale machine, as predicted by that in the model, is 320 kw.

An earlier power measurement was made by the above method; however, a full-scale power loss of 470 kw was predicted. This high value was blamed on excessive use of solder in the fabrication of the model. A

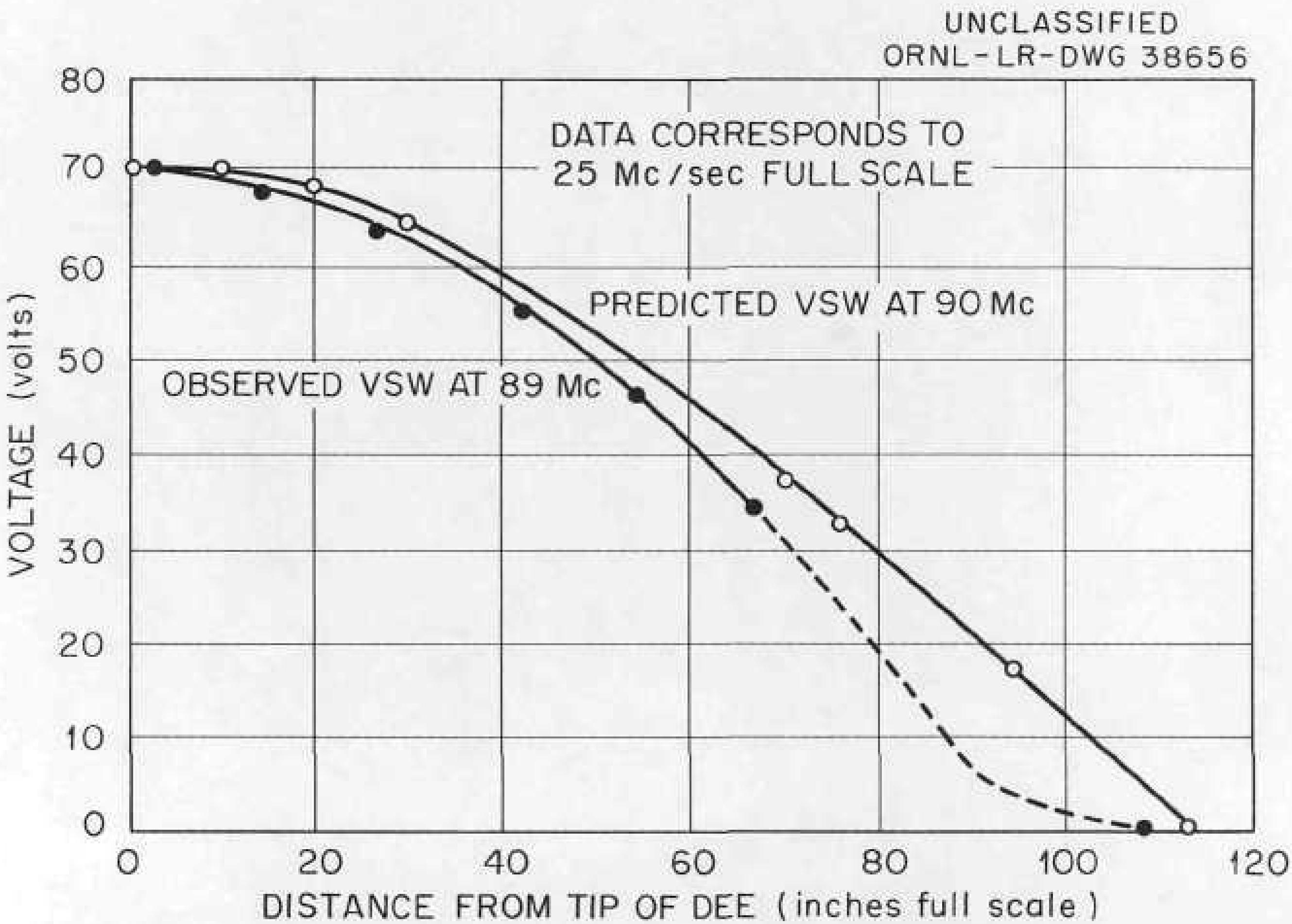

Fig. 16. Measured and Predicted VSW.

new dee was fabricated by improved soldering techniques; the effect on power requirements can readily be seen.

Conclusion

The power loss in the model is nearly 50% greater than the predicted loss of 230 kw. Some extra loss is due to poor contact and solder joints. The discrepancy between the predicted and observed VSW curves, however, shows that the characteristic impedance in the dee region is somewhat lower than the predicted value. Consequently, the current density in the shorting-plane region would be higher than the predicted value, and some increase in power loss will result.

Improvements in the transition-region geometry will improve current distribution, and increase the resonator frequency range. Some reduction of Z_0 along the elliptical section of the dee stem will help reduce the shorting-plane current. With these corrections, it should be possible to approach the predicted power loss of 230 kw.

ABSTRACT NO.: JOURNAL CATEGORY: 85 SERIAL NO. 31311 SJU549

REPORT NO.	REPORT CATEGORY	REPORT CLASS.	P/NP	JOURNAL
CF-59-6-18	C-28	UNCL.	P	NSA

ORIC R-F MODEL III PROGRESS REPORT. R. E. Worsham and S. W. Mosko (Oak Ridge National Lab., Tenn.). June 2, 1959. 36p.

Dep.(mc) $6.30(ph), $3.00(mf) OTS

Accelerators

2-9-61jla

DATE/INITIALS AVAILABILITY

CLASSIFICATION REVIEW

DES. CAT.________ INITIALS________

DES. CAT. AND SUBJECTS________ INITIALS________

ENTIRE FORM________ INITIALS________

☑ ABSTRACT ATTACHED

PERSONAL AUTHOR(S)

SHORT TITLE: Progress Report on ORIC R-F Model III

CORPORATE AUTHOR(S) 70,243

SUBJECT CODE	INDEX ENTRY
✓603 032	ORNL Relativistic Isochronous Cyclotron-- resonator ~~model~~ characteristics & ~~[illegible]~~ radiofrequency-system
✓702 603	Radiofrequency oscillators -- design specifications for Oak Ridge Isochronous Cyclotron

cnl 2/23

4. CARD CATALOG/MASTER FILE

BOG

OTI-70 (1-61)